GE Healthcare

Q.Clear

Steve Ross, Ph.D.

Accurate quantitation (SUV - Standardized Uptake Value) is becoming more important as clinicians seek to utilize PET imaging for more than just diagnosing and staging disease, but also for treatment monitoring. The significant challenge with delivering consistently accurate SUV measurements in PET imaging is that lesion size, volume and contrast recovery are highly impacted by today's reconstruction algorithm. Q.Clear technology is a step forward in providing quantitation accuracy while not sacrificing excellent image quality in PET imaging. This new approach considers all aspects of the imaging chain and the cumulative effect of all improvements, from small to large, to make PET/CT imaging an accurate tool for enabling both confident diagnosis and precise treatment response assessment.

INTRODUCTION

There is renewed interest in the PET imaging community in obtaining quantitative information about lesion uptake values. Because of this, improvements in image reconstruction algorithms that offer the ability to obtain more accurate estimates of uptake in lesions are of significant interest. Many advancements have been made towards this end, including improvements in system corrections such as randoms and fully 3D scatters[1-2], advances in motion correction[3], modeling of the system point spread function[4], and the inclusion of more accurate projectors and the incorporation of all system corrections into a fully 3D PET image reconstruction model[5].

A core tenet of PET image reconstruction algorithms is the modeling of the underlying PET Poisson noise statistics. Iterative image reconstruction techniques that accurately model the inherent PET physics are generally preferred over standard analytic methods including filtered backprojection (FBP) because of significant increases in signal-to-noise (SNR). The most commonly used clinical PET reconstruction algorithm is the Ordered Subsets Expectation Maximization (OSEM) algorithm. OSEM offers the advantage of accurately modeling the underlying PET physics and also generating the PET images in clinically relevant times via accelerated convergence through the use of subsets.

One drawback to the OSEM algorithm is that it generally cannot be run to full convergence because the noise in the image grows with each iteration. To compensate for this, the algorithm is generally stopped after a predetermined number of iterations, typically two to four, resulting in an under-converged image. Because PET contrast recovery depends on OSEM convergence rates, an under-converged image may produce bias, directly impacting lesion quantitation.

To address the effects of convergence and provide more accuracy in PET quantitation, the Regularized Reconstruction iterative algorithm (Q.Clear) is being introduced, incorporating prior knowledge about the image quality into the reconstruction. This prior knowledge is incorporated as a term in the algorithm discouraging differences in neighboring image voxel values. By incorporating this factor into the reconstruction algorithm, the algorithm can be run to full convergence and provide more accurate quantitation levels and improved SNR over OSEM.

OSEM AND CONVERGENCE

The most widely used reconstruction algorithm in PET clinical imaging is OSEM, an accelerated variant of the ML-EM algorithm[6-8]. The goal of ML-EM is to find the most likely image given the data, defined as the image that maximizes the likelihood (or statistical probability) of producing the acquired data. For Poisson data, the goal of maximizing that probability (expressed here as its logarithm) can be described mathematically by the objective function

$$\hat{x} = \arg\max_{x \geq 0} \sum_{i=1}^{n_d} y_i \log[Px]_i - [Px]_i, \qquad (1)$$

where y_i represents the measured PET coincidence data, x is the image estimate, and P is the system geometry matrix.

The ML-EM algorithm provides an update equation which, given an image that isn't at the maximum of this function, generates a new image with an increased likelihood. Repeating, or iterating, this algorithm to convergence, when the update equation does not substantially change the image, yields the ML image. OSEM accelerates the convergence of ML by performing updates based only on a portion of the data at once, which approximates the ML-EM solution in much less reconstruction time.

Due to the low volume of information in a conventional clinical PET acquisition, reconstructions using ML-EM or OSEM suffer from high noise when run to its full convergence. To avoid this result, the algorithm is typically stopped after 2-4 iterations. This is an effective method to reduce noise in the PET images, but the noise reduction comes at a cost of reduced quantitative accuracy and the potential introduction of distortions in small objects.

This effect is demonstrated with a simple simulation as shown in Figure 1. Two small active objects of the same size and activity level are simulated, with one of the small objects placed between the two large elliptical objects of uniform activity distribution. Reconstructed images are shown using OSEM with 2 iterations and 25 iterations. While the fully converged 25 iteration image shows much improved contrast and a significant reduction in spatial distortions, excessive noise is introduced.

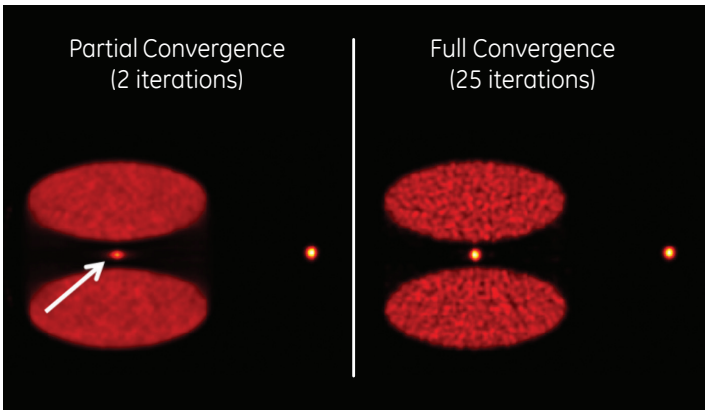

Figure 1. Phantom simulation demonstrating the effects of convergence. The image on the left is reconstructed with two iterations of OSEM; on the right, 25 iterations. Note the spatial distortion and loss of counts in the indicated feature at 2 iterations.

A clinical example of this effect is shown in Figure 2. Excessive noise is introduced into the high iteration images. To avoid this, an under-converged image, like the two-iterations image shown, is typically used in clinical practice.

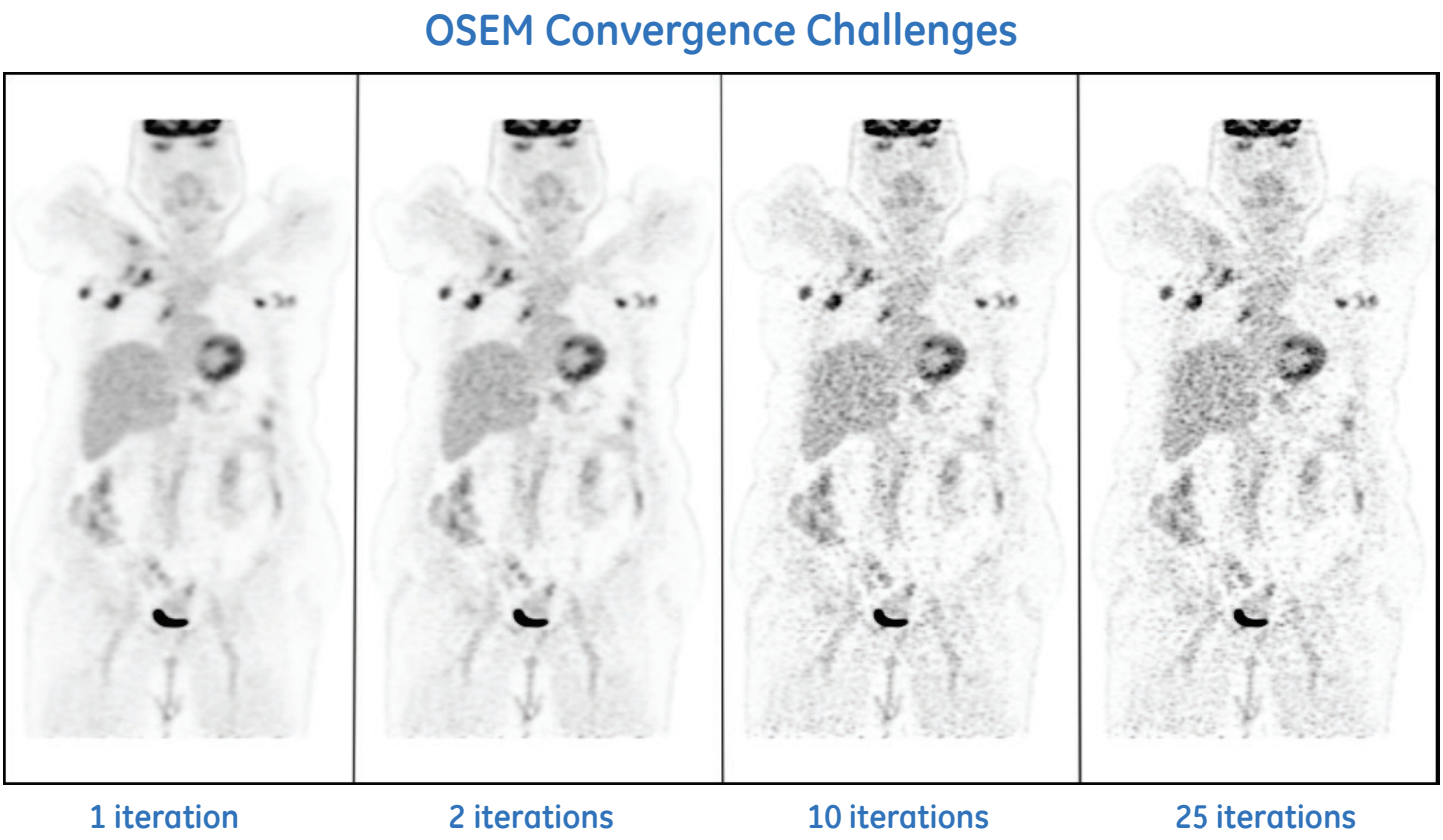

Figure 2. Clinical data reconstructed with a range of OSEM iterations. Excessive noise is introduced as the image reaches convergence.

Q.CLEAR

Q.Clear is a Bayesian penalized likelihood (PL) reconstruction algorithm[9-10] which incorporates an additional term in the objective function of equation 1. This term increases as image noise increases, reducing the objective function, which has the effect of steering the optimization algorithm away from noisier images. This allows the algorithm to reach full convergence without the detrimental effects of excessive noise found with OSEM.

The PL objective function is written as:

$$\hat{x} = \arg\max_{x\geq 0} \sum_{i=1}^{n_d} y_i \log[Px]_i - [Px]_i - \beta R(x), \quad (2)$$

where the first several terms are the same as in Equation 1, *R(x)* is a penalty to control noise and *β* controls the relative strength of the regularizing term relative to the data statistics.

Q.Clear makes use of the Relative Difference Penalty (RDP) [11] which has the advantage of providing activity dependent noise control. The RDP is given by

$$R(\underline{x}) \equiv \sum_{j=1}^{n_v} \sum_{k\in N_j} w_j w_k \frac{(x_j - x_k)^2}{(x_j + x_k) + \gamma\left|x_j - x_k\right|}, \quad (3)$$

where w^j and w^k are relative weights for different components of the function and γ is a tunable parameter which controls edge preservation.

Q.Clear uses the Block Sequential Regularized Expectation Maximization (BSREM) algorithm to solve equation 2[12-13]. BSREM algorithm allows every single image voxel to achieve 100% convergence despite OSEM that did not seek for convergence and may achieve partial convergence, full convergence or over convergence in one single image.

The regularization is also modulated to allow an optimal tradeoff between image quality and quantitation. The penalty is designed such that edges are preserved while background image noise is kept low, thus providing superior image quality[14]. Because Q.Clear is always run to convergence, iterations and subsets are no longer inputs provided to the user as is commonly done in OSEM. In addition, since the image noise is controlled inside the iterative reconstruction as part of regularization, post filters are not necessary; this is shown in the process flow map of Figure 3.

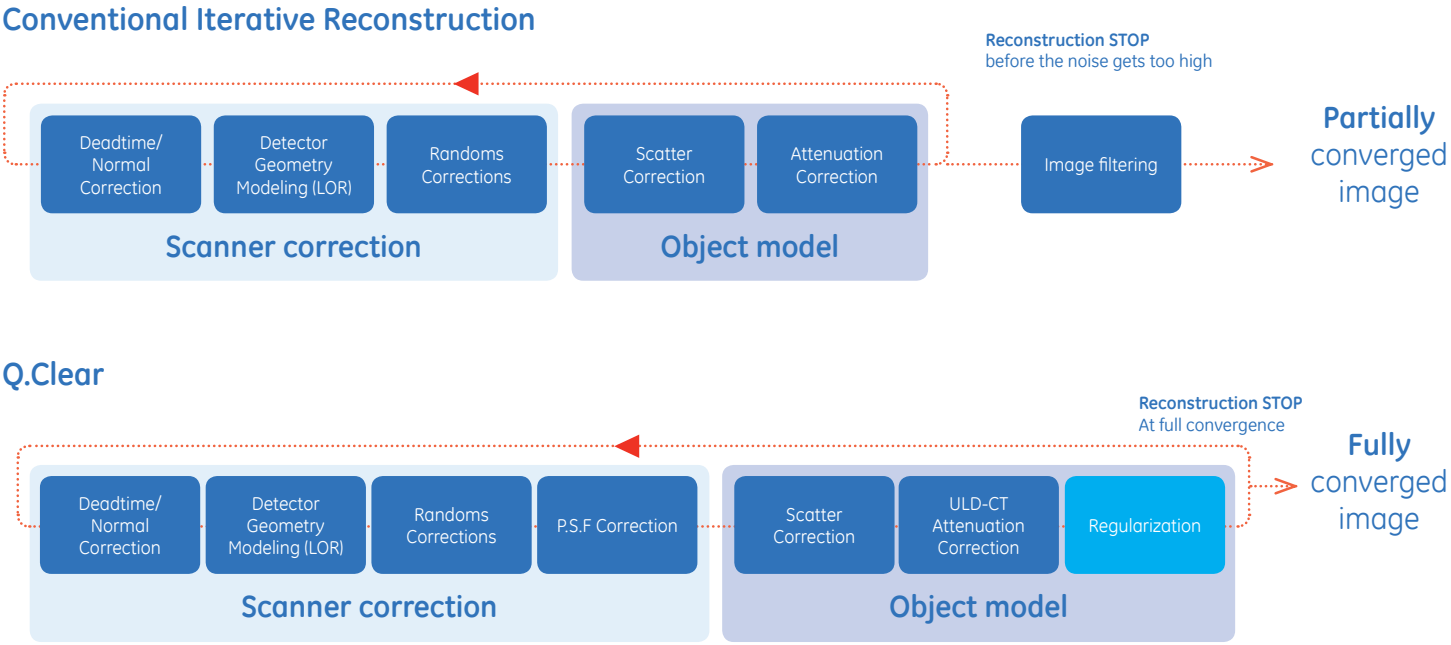

Figure 3. Process flow maps for conventional OSEM iterative reconstruction and Q.Clear. Q.Clear is a fully convergent iterative reconstruction method. Unlike OSEM, Q.Clear controls noise as part of the regularization process inside iterative reconstruction.

FULL CONVERGENCE WITH NO COMPROMISES

PHANTOM ANALYSIS

Anthropomorphic Phantoms

To demonstrate that full convergence using Q.CLEAR doesn't compromise image quality, SNR has been measured on two anthropomorphic phantoms filled and scanned on the Discovery* PET/CT 710. The first phantom was an Anthropomorphic Torso Phantom™ (Data Spectrum Inc, Durham, NC) as shown in Figure 4. The phantom was modified by the manufacturer so that 10 mm diameter hollow spherical inserts could be placed in varying locations within the phantom. The phantom was filled with ^{18}F-FDG and the spheres were filled to a target of four times the background.

The second phantom scanned was a modified Extended Oval Phantom™ (also from Data Spectrum) as shown in Figure 5. The phantom was modified to include two mounted bottles, and each was filled to a similar density as the lung background of the anthropomorphic phantom. In addition, another bottle mounted in the middle of the phantom was filled to twice the background activity in order to emulate a hot organ. The phantom also contained spherical inserts to mimic lesions. These spheres were filled to 4 times the background activity concentration. In the Extended Oval phantom, a 10 mm diameter sphere was placed into one lung insert. In the background, two spheres (10 mm, 13 mm) were located between the lungs and the hot organ (see Figure 4). A 40 million count PET/CT study was done on the Discovery PET/CT 710 scanner to simulate a single frame of a representative clinical exam.

Data acquired from both phantoms was reconstructed with OSEM and Q.Clear. The OSEM images were filtered with a 4 mm transaxial Gaussian filter and a light axial filter [1:6:1] to control noise. The Q.Clear images were reconstructed with β=350 and no post filtering. All corrections were applied inside the iterative reconstruction loop as shown in Figure 3 for both OSEM and Q.Clear. The images reconstructed using Q.Clear, shown in Figure 4 and Figure 5, demonstrate superior contrast to the OSEM images, particularly in the lung region. This is attributed to the slow convergence of OSEM in the cold background. The SNR results demonstrate a significant improvement with Q.Clear over OSEM, with particular improvement shown in the lung region but a clear benefit throughout the entire image.

(a)

(b)

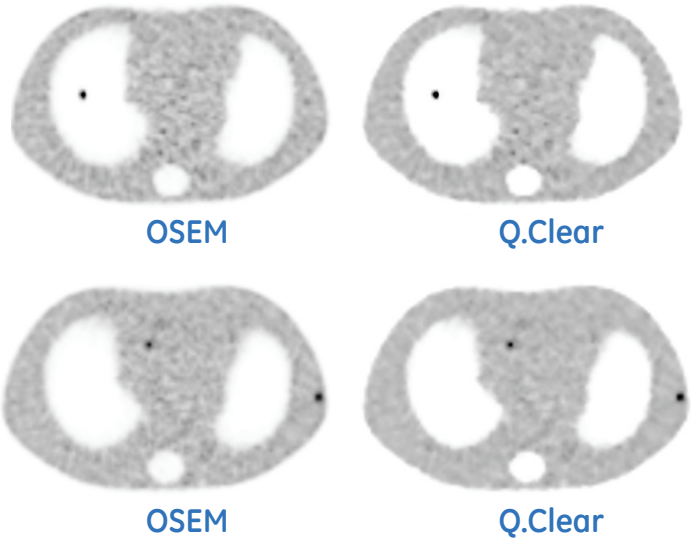

(c)

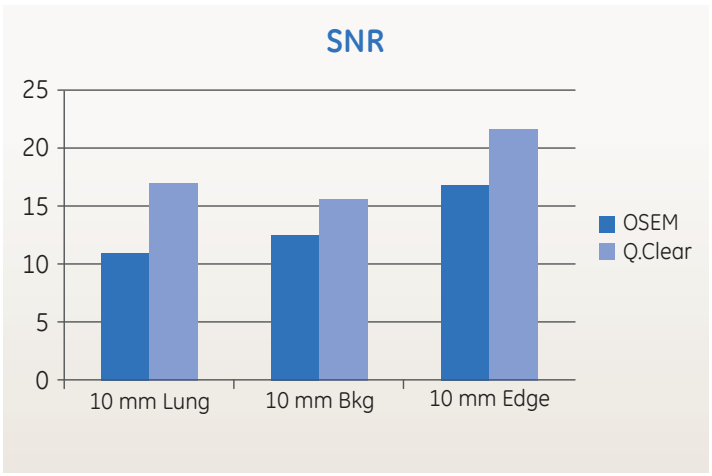

Figure 4. (a) Anthropmorphic Torso Phantom™ (Data Spectrum, Durham, NC) modified to include 10 mm spherical inserts. (b) Reconstructed images from a 40M count study acquired on a Discovery PET/CT 710. OSEM images reconstructed using 2 iterations/24 subsets and a post-filtering of a 4 mm FWHM Gaussian in-plane and a [1:6:1] weighted axial filter. Q.Clear images reconstructed with β=350 and no post filtering. (c) SNR measurements where SNR is defined as signal in a sphere ROI divided by the standard deviation of large uniform background VOI.

(a)

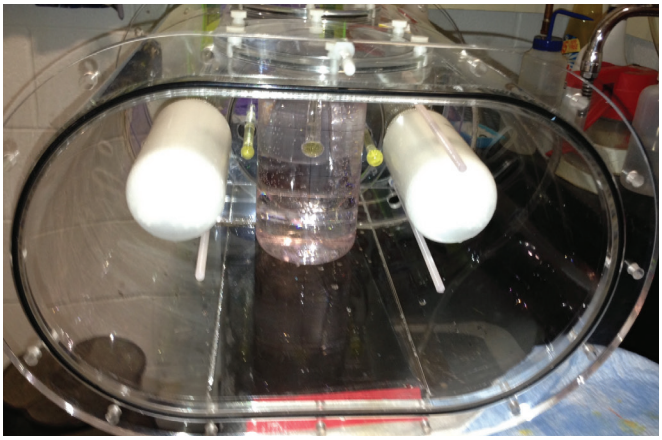

(b)

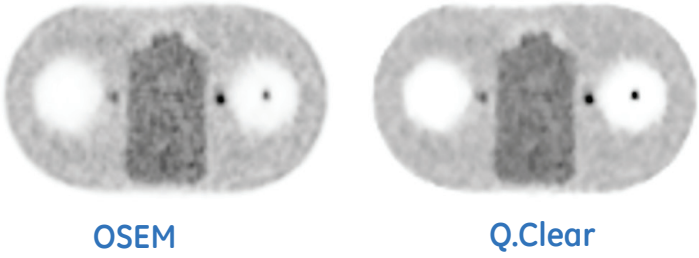

(c)

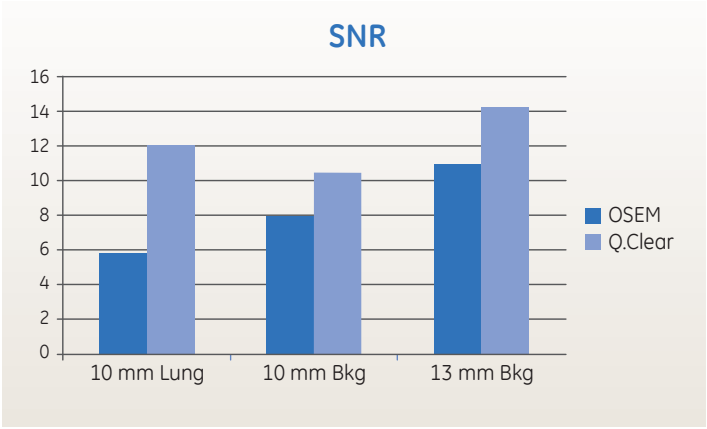

Figure 5 (a) Extended Oval Phantom™ (Data Spectrum, Durham, NC) modified to include 10 mm and 13 mm spherical inserts, a lung region and an adjacent hot organ. (b) Reconstructed images from a 40M count study acquired on a Discovery PET/CT 710. OSEM images reconstructed using 2 iterations/24 subsets and a post-filtering of a 4 mm FWHM Gaussian in-plane and a [1:6:1] weighted axial filter. Q.Clear images reconstructed with β=350 and no post filtering. (c) SNR measurements where SNR is defined as signal in a sphere ROI divided by the standard deviation of large uniform background VOI.

NEMA Image Quality Phantom

A NEMA Image Quality IEC Phantom (Data Spectrum, Durham, NC) shown was filled with ^{18}F-FDG and scanned on the Discovery PET/CT 710. Images were reconstructed with OSEM and Q.Clear. As described previously, all corrections were applied inside the iterative loop for both algorithms. OSEM images with 2 and 25 iterations are shown along with a Q.Clear image in Figure 6. The 25 iteration OSEM image shows improved contrast over the 2 iteration image; however, there is also a significant increase in image noise. Q.Clear shows up to 2 times improvement in PET quantitation accuracy (SUVmean) and PET image quality (SNR) over OSEM on both the Discovery PET/CT 610 and Discovery PET/CT 710.

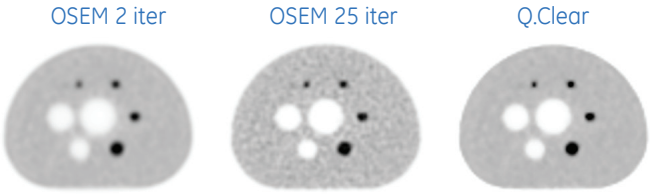

Figure 6. (a) NEMA Image Quality Phantom (Data Spectrum, Durham, NC) images from a study acquired on a Discovery PET/CT 710. OSEM images are shown for 2 iterations and 25 iterations and a post-filtering of a 6.4 mm FWHM Gaussian in-plane and a [1:4:1] weighted axial filter "Standard" axial filter). Q.Clear images are shown with β=350.

QUANTITATION AND VISUAL IMPROVEMENTS ON CLINICAL DATA

PET/CT scans acquired on Discovery PET/CT 690 and Discovery PET/CT 710 systems were reconstructed with OSEM and Q.Clear. All corrections were applied inside the iterative reconstruction loop for both OSEM and Q.Clear. OSEM and Q.Clear reconstructed images are shown in Figures 7, 8 and 9. The images show a significant increase in SUV_{mean} with Q.Clear.

Figure 7 shows whole-body 18^{F}-FDG clinical images acquired on the Discovery PET/CT 690. The OSEM image was reconstructed using 2 iterations/24 subsets and a post-filter of a 4 mm FWHM Gaussian in-plane and a [1:6:1] weighted axial filter. The Q.Clear image was reconstructed with a β=350 and no post filtering.

Figure 8 shows ^{68}Ga-DOTATOC clinical images acquired on a Discovery PET/CT 710, which also demonstrates a significant increase in SUV mean with Q.Clear. The OSEM image was reconstructed using 2 iterations/24 subsets and a post-filter of a 6.4 mm FWHM Gaussian in-plane and a [1:4:1] weighted axial filter. The Q.Clear image was reconstructed with a β=400.

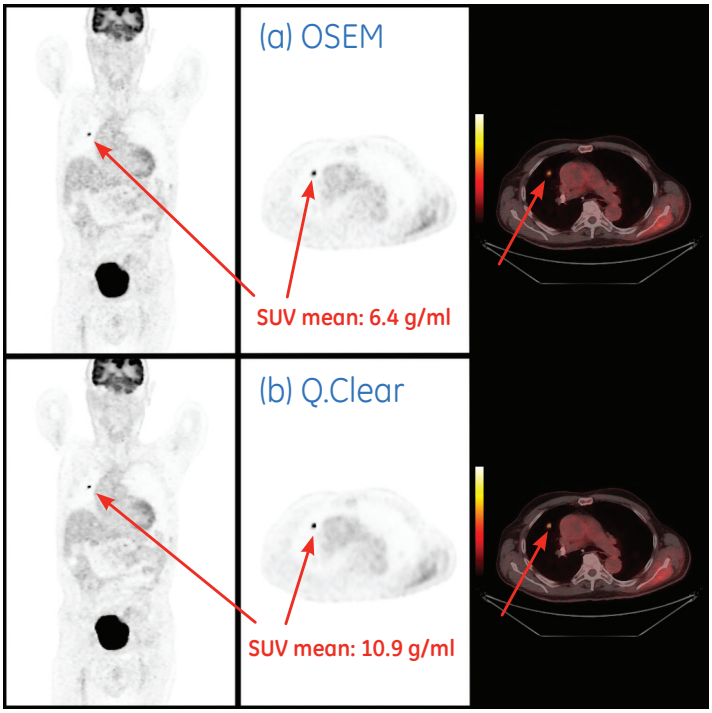

Figure 7. Clinical ^{18}F-FDG images acquired on a Discovery PET/CT 690. The OSEM image was reconstructed using 2 iterations/24 subsets and a post-filtering of a 4 mm FWHM Gaussian in-plane and a [1:6:1] weighted axial filter ("Light" axial filter). The Q.Clear image was reconstructed with β=350.

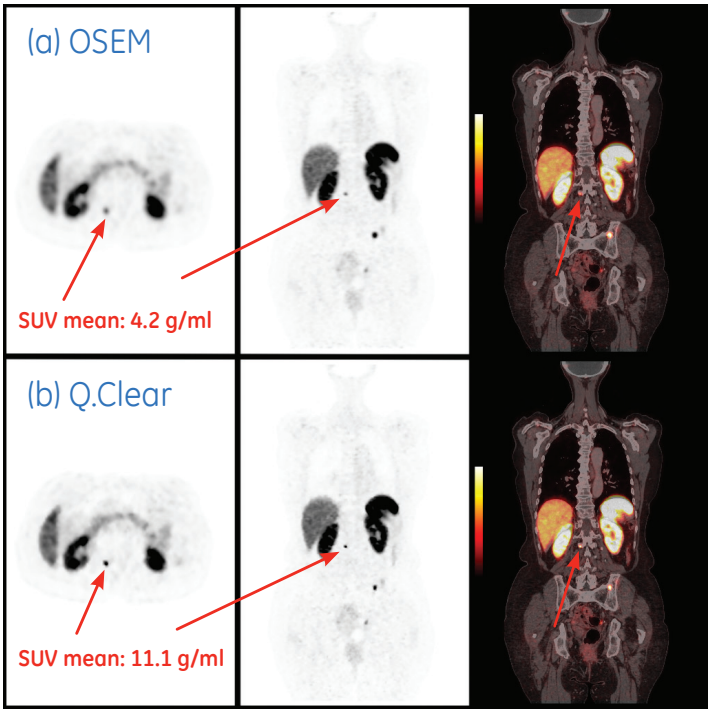

Figure 8. Clinical ^{68}Ga images acquired on a Discovery PET/CT 710. The OSEM image was reconstructed using 2 iterations/24 subsets and a post-filtering of a 6.4 mm FWHM Gaussian in-plane and a [1:4:1] weighted axial filter ("Standard" axial filter). The Q.Clear image was reconstructed with β=400.

Figure 9 shows ^{18}F-FDG clinical images acquired on the Discovery PET/CT 600 which also demonstrates a significant increase in SUV mean with Q.Clear. The OSEM image was reconstructed using 2 iterations/32 subsets and a post-filter of a 6.4 mm FWHM Gaussian in-plane and a [1:4:1] weighted axial filter. The Q.Clear image was reconstructed with a β=200 and no post filtering.

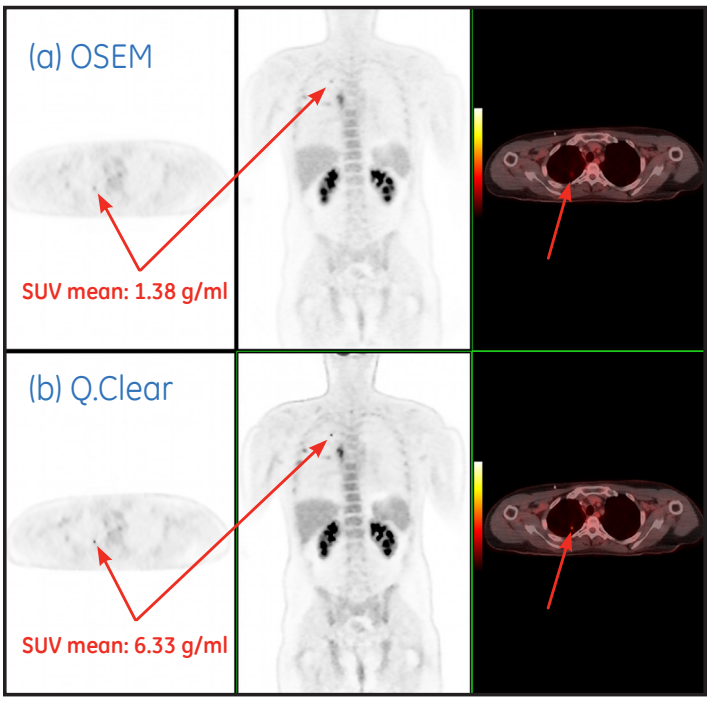

Figure 9. Whole-body ^{18}F-FDG clinical images acquired on the Discovery PET/CT 600. The OSEM image was reconstructed using 2 iterations/32 subsets and a post-filter of a 6.4 mm FWHM Gaussian in-plane and a [1:4:1] weighted axial filter. The Q.Clear image was reconstructed with a β=200 and no post filtering.

Figure 10 shows ^{18}F-FDG brain images from two exams acquired on a Discovery PET/CT 690 and reconstructed with OSEM and Q.Clear. The OSEM images were reconstructed with 3 iterations/32 subsets and a post-filter of 2.5 mm. The Q.Clear images were reconstructed with a β=150 and demonstrate excellent contrast and image quality in both brain exams.

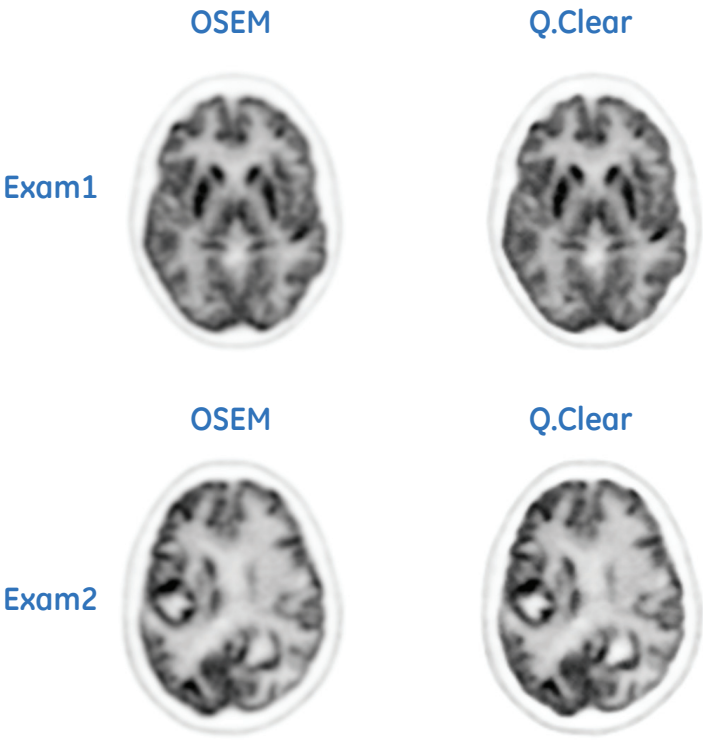

Figure 10. Two clinical ^{18}F-FDG brain acquisitions from a Discovery PET/CT 690. The OSEM images were reconstructed using 3 iterations/32 subsets and a post-filtering of a 2.5 mm FWHM Gaussian in-plane. The Q.Clear images were reconstructed with β=150.

SUMMARY

Many recent advancements have been made towards improved quantitative accuracy in PET imaging. A current impediment towards superior quantitative imaging in PET was the necessary under-convergence required in OSEM to control image noise. Q.Clear provides a fully convergent PET image reconstruction technique, enabled by controlling image noise through regularized reconstruction. Q.Clear was designed to provide excellent image quality and consistent and accurate quantitation.

Like any change in reconstruction processing, the effects of the Q.Clear algorithm should be considered when evaluating longitudinal studies. The results presented here demonstrate that Q.Clear provides an increase in both SNR and SUV recovery over OSEM. As such, Q.Clear is the foundation in the next generation of quantitative imaging.

REFERENCES

[1] C. Stearns, D. McDaniel, S. Kohlmyer, P. Arul, B. Geiser and V. Shanmugam, "Random coincidence estimation from single event rates on the Discovery ST PET/CT scanner," IEEE Nuclear Science Symposium Conference Record, 2003.

[2] M. Iatrou, R. Manjeshwar, S. Ross, K. Thielemans, and C. Stearns, "3D implementation of scatter estimation in 3D PET," IEEE Nuclear Science Symposium Conference Record, 2006, pp 2142-2145.

[3] S. D. Wollenweber, G. Gopalakrishnan, K. Thielemans, and R. M. Manjeshwar, "Evaluation of the Accuracy and Robustness of a Motion Correction Algorithm for PET Using a Novel Phantom Approach," 2012, IEEE Transactions on Nuclear Science, Vol. 59 (1), pp. 123–130.

[4] A. Alessio, C. Stearns, S. Tong, S. Ross, S. Kohlmyer, A. Ganin, P. Kinahan, "Application and evaluation of a measured spatially variant system model for PET image reconstruction," IEEE Transactions on Medical Imaging, 2010, Vol. 29 (3), pp 938-949.

[5] R. Manjeshwar, S. Ross, M. Iatrou, T. Deller, and C. Stearns, "Fully 3D PET iterative reconstruction using distance-driven projectors and native scanner geometry," IEEE Nuclear Science Symposium Conference Record, 2006, pp 2804-2807.

[6] L.A. Shepp and Y. Vardi, Maximum likelihood estimation for emission tomography, IEEE Transactions on Medical Imaging, 1982, Vol 1, pp. 113-121,

[7] K. Lange and R. Carson, "EM reconstruction algorithms for emission and transmission tomography," Journal of Computer Assisted Tomogrphay, 1984, Vol. 8, pp., 306-316.

[8] H.M. Hudson and R.S. Larkin, "Accelerated image reconstruction using ordered subsets of projection data," IEEE Transactions on Medical Imaging, 1994, Vol 16, pp. 516-526.

[9] C-T.Chen, V. E. Johnson, W. H. Wong, X. Hul, and C. E. Metz, " Bayesian Image Reconstruction in Positron Emission Tomography", IEEE Transactions on Nuclear Science, 1990, Vol. 37 (2), pp. 636-641.

[10] E.U. Mumcuoglu, R. Leahy, S.R.Cherry, Z. Zhou, "Fast gradient-based methods for Bayesian reconstruction of transmission and emission PET images", IEEE Transactions on Medical. Imaging, 1994, Vol. 13 (4), pp. 687-701.

[11] J. Nuyts, D. Beque, P. Dupont, L. Mortelmans, "A concave prior penalizing relative differences for maximum-a-posteriori reconstruction in emission tomography", IEEE Transactions on Nuclear Science, 2002, Vol. 49 (1), pp. 56–60.

[12] A. R. De Pierro and M. E. B. Yamagishi, "Fast EM-like methods for maximum 'a posteriori' estimates in emission tomography," IEEE Transactions on Medical Imaging, 2001, Vol. 20, pp. 280–288.

[13] S. Ahn and J.A. Fessler, "Globally convergent image reconstruction for emission tomography using relaxed ordered subsets algorithms," IEEE Transactions on Medical Imaging, 2003, Vol. 22 (5), pp. 613–26.

[14] E. Asma, S. Ahn, S. Ross, A. Chen, and R. Manjeshwar, "Accurate and consistent lesion quantitation with clinically acceptable penalized likelihood images," IEEE Nuclear Science Symposium Conference Record, 2012.

About GE Healthcare

GE Healthcare provides transformational medical technologies and services to meet the demand for increased access, enhanced quality and more affordable healthcare around the world. GE (NYSE: GE) works on things that matter - great people and technologies taking on tough challenges. From medical imaging, software & IT, patient monitoring and diagnostics to drug discovery, biopharmaceutical manufacturing technologies and performance improvement solutions, GE Healthcare helps medical professionals deliver great healthcare to their patients.

GE Healthcare
3000 N Grandview Blvd
Waukesha, WI 53188
USA
www.gehealthcare.com

imagination at work

GE Healthcare, a division of General Electric Company. DOC1474189, Rev 3